HHS Public Access

Author manuscript

Cell Mol Life Sci. Author manuscript; available in PMC 2016 December 01.

Published in final edited form as:

Cell Mol Life Sci. 2015 December ; 72(24): 4849–4866. doi:10.1007/s00018-015-1973-4.

Rab5-mediated VE-cadherin internalization regulates the barrier function of the lung microvascular endothelium

Junjun Yang[1], **Wei Yao**[1], **Guisheng Qian**[1], **Zhenghua Wei**[1], **Guangyu Wu**[2], and **Guansong Wang**[1]

Guangyu Wu: guwu@gru.edu; Guansong Wang: wanggs2003@hotmail.com, wanggs@tmmu.edu.cn

[1]Institute of Respiratory Diseases and Critical Care, Xinqiao Hospital, Third Military Medical University, Chongqing 400037, China

[2]Department of Pharmacology and Toxicology, Medical College of Georgia, Georgia Regents University, 1459 Laney Walker Blvd., Augusta, GA 30912, USA

Abstract

The small GTPase Rab5 has been well defined to control the vesicle-mediated plasma membrane protein transport to the endosomal compartment. However, its function in the internalization of vascular endothelial (VE)-cadherin, an important component of adherens junctions, and as a result regulating the endothelial cell polarity and barrier function remain unknown. Here, we demonstrated that lipopolysaccharide (LPS) simulation markedly enhanced the activation and expression of Rab5 in human pulmonary microvascular endothelial cells (HPMECs), which is accompanied by VE-cadherin internalization. In parallel, LPS challenge also induced abnormal cell polarity and dysfunction of the endothelial barrier in HPMECs. LPS stimulation promoted the translocation of VE-cadherin from the plasma membrane to intracellular compartments, and intracellularly expressed VE-cadherin was extensively colocalized with Rab5. Small interfering RNA (siRNA)-mediated depletion of Rab5a expression attenuated the disruption of LPS-induced internalization of VE-cadherin and the disorder of cell polarity. Furthermore, knockdown of Rab5 inhibited the vascular endothelial hyperpermeability and protected endothelial barrier function from LPS injury, both in vitro and in vivo. These results suggest that Rab5 is a critical mediator of LPS-induced endothelial barrier dysfunction, which is likely mediated through regulating VE-cadherin internalization. These findings provide evidence, implicating that Rab5a is a potential therapeutic target for preventing endothelial barrier disruption and vascular inflammation.

Keywords

Rab5 GTPase; VE-cadherin; Actin cytoskeleton; Internalization; Endothelium; Barrier function; Acute lung injury; Endosome; Adherens junction; Cell polarity

Correspondence to: Guangyu Wu, guwu@gru.edu; Guansong Wang, wanggs2003@hotmail.comwanggs@tmmu.edu.cn.

Electronic supplementary material The online version of this article (doi:10.1007/s00018-015-1973-4) contains supplementary material, which is available to authorized users.

Conflict of interest The authors declare that they have no competing interests.

Introduction

The vascular endothelium is formed by a continuous endothelial cell monolayer, constituting a semi-selective barrier between the blood and the interstitium that controls the exchange of macromolecules and fluid [1]. Endothelial permeability is essential for the inflammation pathogenesis underlying many diseases, such as acute respiratory distress syndrome (ARDS) [2]. Endothelial barrier function is regulated by adherens and tight junctions. The assembly and organization of adherens junctions precede the formation of tight junctions, which have important functions, including the establishment and maintenance of cell–cell adhesion and actin cytoskeleton remodeling. Vascular endothelial (VE)-cadherin is an endothelial-specific transmembrane component of adherens junction complexes that plays key roles in the maintenance of vascular integrity [3, 4], including rearrangement of the cytoskeleton [5], establishment of cell polarity [6], and tight junction remodeling [7].

Cell polarity describes the asymmetric organization of most of the physical structures of the cell, such as the cytoskeleton and organelles [8, 9]. The establishment and maintenance of cell polarity are critical to several cell and tissue functions, including cell division, cell migration, neuronal synaptic transmission, epithelial and endothelial barriers, and lumen formation. There are at least four types of cell polarity: anterior–posterior polarity, migratory polarity, apical–basal polarity, and planar cell polarity (PCP) [10]. It has been well established that a cell polarity complex consisting of partitioning defective 3 (PAR-3), PAR-6, and atypical protein kinase C (aPKC) plays a crucial role in the development of apical–basal polarity in epithelial cells [11–13]. In addition, PAR3 and PAR6 associate directly with VE-cadherin to regulate tight junction integrity [14–17]. Studies have shown that the loss of VE-cadherin causes the mislocalization of PAR3 and abnormal endothelial cell polarity [6]. However, the relationship between cell polarity and VE-cadherin in microvascular cells, especially regarding the regulation of endothelial permeability, remains unclear.

Members of the Rab GTPases are localized to various intracellular compartments, where they control vesicular trafficking through their interactions with specific tethering proteins and the cytoskeleton [18, 19]. Among the Rab GTPases, Rab5 localizes to early endosomes, the plasma membrane, and clathrin-coated vesicles and is involved in the control of intracellular trafficking, largely between the plasma membrane and the endosomal compartment [19]. Rab5 has three isoforms, Rab5a, Rab5b, and Rab5c [20]. In addition to its role in endocytosis, Rab5 has been implicated in other cellular processes, such as cell adhesion and migration, cell mitosis, autophagy, and so on [21–24]. As an important isoform of Rab5, Rab5a plays a crucial role in the internalization of plasma membrane proteins and their return to the cell surface. It not only regulates G protein-coupled receptor (GPCR) trafficking, but also mediates junction protein localization [25–29]. However, the effect of Rab5a on VE-cadherin internalization and EC polarity is not clear. The relationships between the expression of Rab5a and that of VE-cadherin and between Rab5a and cell polarity also remain poorly understood.

In this study, we investigated whether Rab5a is involved in LPS-induced endothelial barrier dysfunction. Through knockdown or overexpression of Rab5a, we determined its ability to

mediate endothelial permeability. We also examined the role of Rab5a in regulating the cell polarity of HPMECs. Our results demonstrated that Rab5a is a key mediator of LPS-induced vascular hyperpermeability. In addition, we describe a novel role of Rab5a in the regulation of VE-cadherin internalization and cell polarity in HPMECs. Finally, using an in vivo model of sepsis, we found that silencing Rab5a expression prevents lung endothelium dysfunction caused by LPS injury.

Materials and methods

Reagents

The following were used: LPS from *Escherichia coli* O111:B4, O55:B5, thrombin, and TNF-α (Sigma Aldrich, USA); X-tremeGENE siRNA Transfection Reagent and X-tremeGENE HP DNA Transfection Reagent (Roche, Switzerland); EntransterTM-in vivo transfection reagent (Engreen Biosystem, China); rhodamine-phalloidin (Invitrogen, USA); Rab5a activation assay kit (NewEast Biosciences, USA); FITC-dextran and chloroquine (Santa Cruz, USA); rabbit anti-VE-cadherin, anti-Podxl, goat anti-VE-cadherin, and mouse anti-CD31 (Santa Cruz, USA); rabbit anti-Rab5 (ABCam, USA); rabbit anti-β-actin (Cell Signaling Technology, USA); rabbit anti-F-actin and anti-GAPDH (Biosynthesis Biotechnology, Beijing, China); Alexa Fluor 488- or Alexa Fluor 594-labeled and HRP-coupled goat anti-mouse and anti-rabbit IgG and Dylight 649-donkey anti-goat IgG (ZSGB-Bio, Beijing, China).

Cell line

The human pulmonary microvascular endothelial cells (HPMECs) were purchased from ScienCell Research Laboratories (ScienCell, USA) and cultured in endothelial cell medium (ECM) (ScienCell, USA). The culture medium was supplemented with 1 % endothelial cell growth supplement (ECGS), 1 % penicillin/streptomycin solution (P/S), and 5 % fetal bovine serum (FBS). HPMECs were used for the experiments from passage 3 to passage 10. To obtain polarized cells, HPMECs were trypsinized and seeded on Corning Transwell clear polyester membrane inserts with a pore size of 0.4 μm and 6.5 mm-diameter inserts in 24-well plates. The cells were seeded at a density of 1×10^5 cells/cm^2 with 1.5 ml of ECM medium in the basolateral compartment and 0.5 ml in the apical compartment. The HPMECs were grown as a monolayer, serum-starved (1 % serum) for 2 h, and then exposed to LPS at the indicated concentration for the selected period.

Transfection of Rab5 small interfering RNA (siRNA)

siRNAs targeting human and mouse Rab5a genes [30] and scrambled siRNA were synthesized and purchased from Shanghai GenePharma Co. Ltd. Target sequences were as follows: Rab5a (human) GCCAGAGGAAGAGGAGTAGACCTTA; Rab5a (mouse) GCAACAAGACCCAACGGGCCAAATA. For all the siRNA experiments, the appropriate scrambled oligos were used as negative control siRNAs (NC siRNA).

1. Rab5a siRNA treatment in vitro. HPMECs were transfected with siRNAs using Roche X-tremeGENE siRNA Transfection Reagent according to the manufacturer's instructions. Briefly, X-tremeGENE siRNA Transfection Reagent (20 μL) and the

siRNA (10 μg) were diluted in 200 μL of OPTI-MEM medium (in the absence of antibiotics or fungicides) in separate tubes. These tubes were combined within 5 min, mixed, and incubated for 20 min at 15–25 °C. Finally, the transfection mixture was added to the culture dishes. After 48 h of transfection, the cells were used in experiments. The efficacy of Rab5a knockdown was determined by immunoblotting.

2. Rab5a siRNA treatment in vivo. 2′-OMe-modified siRNAs were used in vivo. Six- to 8-week-old male C57BL/6 mice were injected via the tail vein with 5OD/20 gbw of Rab5a siRNA or scrambled siRNA on day 1. EntransterTM-in vivo transfection reagent was used to deliver the siRNAs according to the manufacturer's recommendations. Then mice were intraperitoneally administered 20 mg/kg LPS or normal saline on day 5. Mice were killed on day 6 for 24 h after LPS challenge. Lung tissues were immediately removed and frozen in liquid nitrogen.

Plasmid transfection

The HPMECs were transfected with the GFP–Rab5a plasmid or the empty plasmid using X-tremeGENE HP DNA Transfection Reagent according to the manufacturer's instructions. Briefly, X-tremeGENE HP DNA Transfection Reagent (1 μL) and the plasmid (0.5 μg) were diluted in 50 μL of OPTI-MEM medium (in the absence of antibiotics or fungicides). The mixture was incubated for 30 min. Finally, the transfection mixture was added to the culture dishes. After 48 h, the cells were processed for fluorescence microscopy.

Sepsis model

All animal experiments were approved by and performed in compliance with the guidelines of the Ethics Committee of Xinqiao Hospital affiliated with Third Military Medical University. Six- to 8-week-old male C57BL/6 were purchased from Beijing HFK Bioscience CO., LTD (Beijing, China) and maintained in specific pathogen-free conditions in the Animal Research Center of Xinqiao Hospital affiliated with Third Military Medical University. C57BL/6 mice with or without transfection with Rab5a siRNA were challenged with 20 mg/kg LPS i.p. on day 5. Mice were killed 24 h after LPS challenge. Lung tissues were immediately removed and frozen in liquid nitrogen. The tissues were embedded in Optimal Cuttin Temperature (OCT, SAKURA, USA) and sections (7 μm) were cut from the blocks, followed by fixing with 4 % paraformaldehyde for 20 min, and then used for fluorescence microscopy, as described below. For histology, paraffin-embedded tissue sections (4 μm) were treated with H&E stain. For the survival studies, the mice were challenged with 40 mg/kg LPS i.p. and then monitored four times daily for 5 days.

Confocal microscopy and image analysis

HPMECs cultured for 6 days on transwell inserts (0.4 μm pore size, Corning, USA) were starved for 2 h in 1 % serum ECM and stimulated with 1 μg/ml LPS for 6 h. After stimulation, cells were briefly washed with phosphate-buffered saline (PBS) and fixed in 4 % paraformaldehyde for 30 min at 4 °C, permeabilized with 0.1 % Triton X-100 for 10 min, and blocked with PBS containing 2 % BSA for 1 h at room temperature. The cells and murine lung tissues sections were stained with specific antibodies, including anti-VE-

cadherin, anti-Rab5a, or anti-Podxl antibodies at 4 °C overnight, followed by species-matched fluorescent secondary antibodies conjugated with Alexa Fluor 594, Alexa Fluor 488, or Dylight 649. To visualize F-actin, HPMECs were stained with rhodamine-phalloidin for 30 min. The nuclei were labeled with 4′, 6-diamidino-2-phenylindole (DAPI). After mounting in anti-fade mounting media, the cells were viewed and photographed with Leica confocal microscopy (Leica microsystems, Germany). Intracellular gap area and the apical/basal fluorescence intensity of the Podxl protein were calculated with Image J software (National Institute of Health, USA). Quantification of the F-actin fluorescence intensity was analyzed by using Leica LAS AF 2.3.0 software (Leica microsystems, Germany).

VE-cadherin internalization assay

HPMECs were cultured for 6 days on transwell inserts (0.4 μm pore size, Corning, USA) and starved for 2 h in 1 % serum ECM. For the VE-cadherin internalization assay, HPMECs were lableled with a goat anti-VE-cadherin extracellular domain antibody (VE-cadherin-*N*) at 4 °C for 1 h as previously described [37]. After washing with ice-cold culture medium to remove unbounded antibodies, HPMECs were treated with 100 μM chloroquine (to inhibit degradation of internalized VE-cadherin) with or without 1 μg/ml LPS for 6 h. Then the cells were washed with PBS and processed for immunofluorescence staining.

Western blotting

Total protein extracts were prepared using M-PER protein extraction reagent (Thermo Fisher Scientific, USA) in the presence of proteinase inhibitor mixture (Thermo Fisher Scientific). Membrane and cytoplasmic protein extracts were prepared using a Membrane and Cytoplasmic Protein Extraction kit (Beyotime, Jiangsu, China). Western blotting was carried out as described previously [31]. Protein samples were separated by 12 % SDS-PAGE and transferred onto polyvinylidene difluoride membranes. The signal was detected by enhanced chemiluminescence detection system (SuperSignal West Pico, Thermo Fisher Scientific, USA). Densitometric analysis was performed using QuantiScan software.

iCELLigence system analysis

The iCELLigence system (ACEA, San Diego, USA) is a cell-based label-free instrument that measures in real-time electrical impedance across gold microelectrodes integrated on the bottom of culture E-plates. HPMECs were seeded in 5 % FBS ECM at a density of 5×10^4 cells per cm in eight-well E-Plates. After cell adhesion, the siRNA transfection mixture was added and cells were cultured for 2 days. As indicated, the cells were allowed to grow until a plateau was reached, typically 72 h after seeding, and were then exposed to various conditions, as described for each experiment. Impedance measurement was displayed in real time as a cell index (CI, an arbitrary unit) by the iCELLigence RTCA software (ACEA, San Diego, USA). The results are presented as mean values of NCI ± SE against time in each condition.

Endothelial cell permeability assay

HPMECs were grown to confluence on 0.4-μm Transwell inserts. The paracellular permeability of 70 kDa FITC-dextran was assessed after stimulation as described previously.

Briefly, after stimulation with 1 μg/ml LPS for different time intervals (1,6, and 12 h), 1 mg/ml FITC-dextran was added to the upper wells. After incubation for 0.5 h, 50 μl medium from the bottom chamber was aspirated into a 96-well plate. Finally, the 96-well plates were evaluated in a fluorescence plate reader with an excitation wavelength of 488 nm and an emission wavelength of 520 nm.

Pulmonary transvascular flux measurement by Evans blue albumin

The assay was carried out as described [32]. To assess vascular leakage, 40 mg/kg Evans blue albumin (EBA) was injected into the tail vein of the mice 2 h before the termination of LPS treatment. Intravascular EBA was washed out by PBS perfusion through the right ventricle for 5 min. Mouse lungs were excised, weighed, homogenized in PBS (1 ml per 100 mg of lung tissue), and followed by addition of two volumes of formamide for 24 h at 60 °C. Evans blue content was determined by OD620 and OD740 of the formamide extract.

Statistical analysis

Data are presented as mean ± SE. Statistical analysis was performed using one-way analysis of variance (ANOVA) and log-rank test to determine statistical significance with p value set at <0.05.

Results

Enhanced expression of Rab5 and dysfunction of the endothelial barrier in HPMECs after LPS treatment

LPS increases Rab5a activity and expression in HPMECs—We first investigated the effect of LPS on the expression and localization of Rab5a in HPMECs. HPMECs were challenged with LPS for various time intervals (0, 1, 6, and 12 h). The activation of Rab5a (Rab5a-GTP) was determined using a pulldown assay, and the expression of Rab5a protein was assessed by Western blot using an anti-Rab5a polyclonal antibody. The activity and expression of Rab5a were significantly increased after LPS challenge for 1, 6, and 12 h (Fig. 1a, b). The levels of active Rab5a were increased to 1.66-fold, 2.01-fold, and 3.15-fold in the 1, 6, and 12 h group, respectively, compared with the 0 h group ($p < 0.05$, Fig. 1b). Rab5a expression after 6 h LPS challenge was also augmented by approximately 1.5-fold compared with the 1 h group ($p < 0.05$, Fig. 1a, b). There was no significant difference in the protein levels of Rab5a following 1 and 12 h of LPS treatment ($p > 0.05$). We also found that the activity and expression of Rab5a was increased by other inflammatory agents, including thrombin and TNF-α (Suppl. Figure 1). The levels of active and total Rab5a obviously increased to 2.48- and 2.12-fold after stimulation with thrombin for 0.5 h, compared with the control group (Suppl. Figure 1A). TNF stimulation for 5 min strongly enhanced the activation of Rab5a without altering the total expression of Rab5a, whereas TNF stimulation for 30 and 180 min consistently increased both the activation and the total expression of Rab5a (Suppl. Figure 1B). We then detected the effect of LPS stimulation on the localization of Rab5a in HPMECs using immunofluorescence methods. The results showed that Rab5 was predominantly localized at the transport vesicles and less at the control cell plasma membrane. After LPS stimulation, the fluorescence intensity of Rab5a was obviously increased in both the cytoplasm and the membranes of HPMECs compared with control

cells (Fig. 1c). These data demonstrate that LPS increases Rab5a activity and expression in HPMECs.

LPS induces the internalization of VE-cadherin and the rearrangement of actin cytoskeleton of HPMECs

We examined the effects of LPS stimulation on the expression and distribution of VE-cadherin and F-actin in cultured HPMECs (Fig. 2). First, we detected the expression of VE-cadherin and F-actin protein after LPS challenge via WB. As shown in Fig. 2a, VE-cadherin was primarily located at the membrane fraction, which was clearly decreased by LPS stimulation. After LPS treatment, VE-cadherin expression in the membrane fraction was decreased by 27.1, 54.1, and 36.3 % after LPS stimulation for 1, 6, and 12 h, respectively. VE-cadherin expression in the membrane fraction was also reduced by 37.1 % in the 6 h group compared to the 1 h group ($p < 0.05$, Fig. 2b). There was no significant difference in the membrane protein level of VE-cadherin between 1 and 12 h of LPS treatment ($p > 0.05$), while the cytosolic levels of VE-cadherin was increased to 1.7-fold or 4.4-fold than that in the control group at 1 or 6 h after treatment ($p < 0.05$, Fig. 2c). In contrast, LPS stimulation did not alter the total amounts of VE-cadherin as well as the expression of F-actin (Fig. 2a). These results suggest that LPS induces VE-cadherin internalization.

Second, we used immunofluorescence microscopy to analyze the LPS-induced morphological changes in HPMECs. HPMEC monolayers were cultured on Transwell inserts and stimulated with 1 μg/ml LPS for 6 h. Under control conditions, VE-cadherin appeared as a continuous line along the interendothelial cell border. Immunostaining for F-actin with rhodamine-phalloidin revealed a predominance of circumferential actin bundles and few stress fibers. After LPS challenge for 6 h, VE-cadherin immunostaining was interrupted and reduced, leading to the formation of intercellular gaps (indicated with arrows, Fig. 2c). In parallel, LPS-induced F-actin reorganization and intercellular gap formation and increased stress fiber formation (arrows indicate intracellular gaps, and arrowheads indicate stress fibers, Fig. 2d). These results demonstrate that LPS induces VE-cadherin disassembly and actin cytoskeleton remodeling in endothelial cells, thereby disrupting endothelial barrier integrity.

LPS causes endothelial barrier dysfunction

Furthermore, we used the ACEA iCELLigence system to monitor the cell index (CI), which represents the endothelial barrier function. The results showed that the normalized CI gradually decreased from 0 h to 12 h after 1 μg/ml LPS challenge (Fig. 3a). The normalized CI of EC decreased to 0.921 of control cells at 1 h. In the 6 and 12 h groups, the normalized CI decreased more significantly after LPS treatment (CI 0.624 and 0.638, respectively; $p < 0.05$ compared with either baseline or 1 h, Fig. 3b). Additionally, we detected LPS-induced endothelial hyperpermeability by measuring the passage of FITC-dextran across the endothelium. As shown in Fig. 3c, the endothelial permeability was obviously enhanced after LPS stimulation. At 1 h, FITC-dextran permeability was increased to 1.41-fold of the control group ($p > 0.05$). FITC-dextran permeability was increased to 3.29-fold, and 2.79-fold in 6 and 12 h groups, respectively, compared with the control group ($p < 0.05$, Fig. 3c). Taken together, these data demonstrate that LPS disrupts endothelial barrier function.

Rab5a regulates VE-cadherin internalization in HPMECs after LPS treatment

To determine the role of Rab5a in regulating endothelial barrier function, we first studied the effects of siRNA-mediated depletion or increased expression of Rab5a on VE-cadherin internalization and actin cytoskeleton reorganization in HPMECs. As shown in Fig. 4a, Cy3-tagged Rab5a siRNA and GFP-tagged Rab5a WT localized to the perinuclear region and the cytoplasm of HPMECs. Based on the fluorescence signal, the transfection efficiencies were between 70 and 90 %. The expression of Rab5a as determined using an anti-Rab5a polyclonal antibody was significantly decreased by 74.8 % in Rab5a siRNA-transfected cells compared to the control or NC siRNA cells. Furthermore, WB also revealed that exogenously GFP–Rab5a was highly expressed in Rab5a plasmid-transfected cells and the expression of GFP–Rab5a did not alter the expression level of endogenous Rab5a (Fig. 4b).

Rab5a modulates the LPS-induced disruption of VE-cadherin in HPMECs

To investigate the role of Rab5a in regulating endothelial barrier function, we first determined the effect of manipulating the expression levels of Rab5a on the LPS-induced VE-cadherin disruption. We found that neither knockdown nor overexpression of Rab5a had any obvious effects on the total VE-cadherin expression (Fig. 5a). However, the LPS-induced decrease in the membrane fraction of VE-cadherin was significantly reversed by Rab5a siRNA transfection. The data indicated that the expression of VE-cadherin in the cell membrane was dramatically reduced to 44.1 % of that in the controls, and the cytosolic VE-cadherin levels increased to 77.0 %, in response to LPS-alone treatment ($p < 0.05$, Fig. 5b). However, pretransfection with Rab5a siRNA followed by LPS treatment could effectively prevent the loss of VE-cadherin from the membrane, which decreased to 75.9 % of that in the control cells; while the cytosolic VE-cadherin levels decreased to 46.1 % ($p < 0.05$, compared with the control and LPS-alone groups). VE-cadherin expression in the cell membrane of the Rab5a overexpression plus LPS group was markedly reduced to 61.2 % of that in the controls ($p < 0.05$).

Fluorescence imaging analysis was conducted to examine barrier dysfunction in HPMECs, which was characterized by the formation of intercellular gaps (Fig. 5c). After stimulation with LPS, similar to the aforementioned changes in VE-cadherin, VE-cadherin expression was reduced, leading to the marked intracellular gap formation in the NC siRNA plus LPS group, the NC plasmid plus LPS group, and the Rab5a WT plasmid plus LPS group (indicated with arrows). In comparison, HPMECs transfected with Rab5a siRNA showed minimal effects on the barrier integrity. The area of intercellular gaps was quantified (Fig. 5d) and shown to be 0.846, 1.377, 1.639, and 2.291 % in the NC siRNA group, Rab5a siRNA group, NC plasmid, and Rab5a WT group, respectively. There was no significant difference compared with the NC siRNA group ($p > 0.05$). After LPS treatment, the area of intercellular gaps was increased in all groups. It was 9.979, 4.380, 10.487, and 11.771 % in the NC siRNA plus LPS group, Rab5a siRNA plus LPS group, NC plasmid plus LPS group, and WT Rab5a plus LPS group, respectively. However, pretransfection of Rab5a siRNA before LPS stimulation markedly inhibited the formation of intercellular gaps compared with that of LPS alone ($p < 0.05$). These results suggest that Rab5 siRNA can protect the localization of VE-cadherin from LPS injury in HPMECs.

Rab5a adjusts the cell actin cytoskeleton remodeling after LPS treatment

At the same time, we monitored the role of Rab5a in LPS-induced F-actin remodeling in HPMECs via transient transfection of Rab5a siRNA or the Rab5a WT plasmid. As shown in Fig. 5e, LPS induced F-actin reorganization, stress fiber formation, cell retraction, and gap formation compared with control cells (arrows indicated with stress fiber). Conversely, Rab5a siRNA prevented LPS-induced stress fiber formation and decreased intercellular gaps. However, transfection of the WT Rab5a plasmid caused an increase in stress fibers and lamellipodia, which also aggravated LPS-induced stress fiber increase and gap formation. These results prove the regulation of Rab5a on LPS-induced F-actin reorganization and endothelial barrier function.

Knockdown of Rab5a suppresses the LPS-induced internalization of VE-cadherin in HPMECs

To investigate the effect of Rab5a in regulating LPS-induced VE-cadherin internalization, we executed VE-cadherin internalization assay. As shown in Fig. 6, LPS stimulation promotes the translocation of extracellular VE-cadherin from the cell membrane to intracellular organelles and intracellularly expressed VE-cadherin is extensively colocalized with Rab5 (Fig. 6, 2nd panel). Furthermore, we have shown that siRNA-mediated depletion of Rab5 markedly inhibits the translocation of VE-cadherin in response to LPS stimulation (Fig. 6, lower panel). These data suggest that LPS can induce the internalization and colocalization of VE-cadherin with Rab5a; therefore, VE-cadherin internalization is likely mediated via a Rab5 pathway.

Rab5a can control the cell polarity of HPMECs

In addition to the role of Rab5a in LPS-induced VE-cadherin and F-actin disruption, we also determined the effect of Rab5a on endothelial cell polarity. After challenge with LPS, we detected the localization of the apical marker podocalyxin (Podxl) via confocal immunofluorescence and then compared its apical versus basal expression in HPMECs. Images obtained along the x/z-axis showed that LPS impaired the apical distribution of Podxl. Transient transfection with Rab5a siRNA inhibited the LPS-induced abnormal distribution of Podxl, whereas the WT Rab5a plasmid did not have this effect (Fig. 7a). The quantitative results of the apical versus basal expression of Podxl are shown in Fig. 7b. In NC siRNA, Rab5a siRNA, and NC plasmid cells, Podxl was highly expressed in the apical membrane with apical/basal ratios of 2.60, 2.27, and 2.30, respectively. The apical/basal ratio of Podxl was decreased to 1.51 in the Rab5a-transfected cells ($p < 0.05$, compared with the NC plasmid group). After stimulation with LPS, the polarization of Podxl expression was significantly decreased in NC siRNA-, NC plasmid- and WT Rab5a plasmid-transfected cells with the apical/basal ratios 1.21, 1.12, and 0.95, respectively ($p < 0.05$, compared with the respective control groups). However, Rab5a knockdown significantly inhibited the LPS-induced abnormal polarization of Podxl (apical/basal ratio: 1.94, $p < 0.05$, compared with the NC siRNA plus LPS group).

To further investigate the role of Rab5a in the LPS-induced disruption of endothelial cell polarity, we measured the distribution of F-actin in Rab5a siRNA and WT Rab5a cells following LPS treatment. As shown in Fig. 7c, NC siRNA, Rab5a siRNA, and NC plasmid

cells presented clear transcellular F-actin fibrils. After LPS stimulation, the cells exhibited a clear absence of transcellular F-actin fibrils, along with a loss of lateral cellular polarity in NC siRNA, NC plasmid, and Rab5a WT cells. However, following the Rab5a siRNA plus LPS treatment, the cells presented a nearly normal cellular polarity and clear transcellular F-actin fibrils. These results suggest that Rab5a siRNA can inhibit the LPS-induced disruption of human endothelial cell polarity.

Knockdown of Rab5a maintains the cell barrier function from LPS stimulation

To address the role of Rab5a in regulating endothelial barrier function, we studied the effects of Rab5a knockdown on the cell index in HPMECs. As shown in Fig. 8a, b, Rab5a depletion markedly inhibited LPS-induced endothelial barrier dysfunction. Rab5a depletion had no effect on the normalized CI of endothelial cells compared with control cells. The normalized CI decreased after the addition of LPS to HPMECs transfected with either NC siRNA or Rab5a siRNA. The addition of LPS to NC siRNA cells resulted in a significant decrease of the NCI to 0.622 at 6 h ($p < 0.05$, compared with the control group). However, the NCI of Rab5a-depleted endothelial cells decreased moderately to 0.789 at 6 h post-LPS addition, and there was significant difference compared with the NC siRNA plus LPS group ($p < 0.05$), indicating that Rab5a expression contributes to the prevention of LPS-induced endothelial barrier dysfunction. Consistent with the CI detection, the results of an FITC-dextran permeability assay demonstrated that endothelial permeability was obviously enhanced to 3.46-fold compared with the control group after LPS stimulation ($p < 0.05$, Fig. 8c). FITC-dextran permeability was increased to 2.06-fold of control group after pretransfection with Rab5a siRNA followed by stimulation with LPS ($p < 0.05$, compared with control group or NC siRNA + LPS group). These results support that knockdown of Rab5 can prohibit LPS-induced endothelial barrier dysfunction.

Suppression of Rab5a can protect the lungs' endothelial barrier function from LPS injury

LPS elevates Rab5a expression in the lung endothelium in vivo—To investigate the influence of LPS on Rab5a in vivo, we detected the localization and expression of Rab5a in the lung endothelium of C57BL/6 mice following intraperitoneal (i.p.) injection of LPS (20 mg/kg). Through immunofluorescent colocalization with the endothelial marker protein CD31, we confirmed the presence of Rab5a in the lung endothelium (Fig. 9a). In addition, Rab5a expression was increased to 2.47-fold in lung tissues after LPS stimulation compared with untreated mice ($p < 0.05$, Fig. 9b), suggesting that LPS increases Rab5a expression in vivo.

Rab5a knockdown inhibits LPS-induced endothelial barrier dysfunction in vivo—Because LPS induced Rab5a expression in vivo (Fig. 9), we next determined whether Rab5a knockdown attenuated LPS-induced endothelial barrier dysfunction and lung injury. First, Cy3-labeled siRNA targeting mouse Rab5a was injected into C57BL/6 mice to specifically knock down Rab5a expression. Confocal microscopy showed that Cy3-expressing cells were detected in lung, kidney, and liver tissues 6 days after transfection (Fig. 10a, Suppl. Figure 2). Furthermore, WB revealed that Rab5a expression in lung tissues was significantly decreased by 62.0 or 69.3 % after Rab5a siRNA transfection for 3 or 6 days, respectively ($p < 0.05$, compared with the control group, Fig. 10b). LPS injection

caused infiltration of Evans blue-stained albumin from the vessel into the lung tissue, further substantiating the effect of LPS on EC barrier dysfunction (Fig. 10c). We also observed that Rab5a siRNA inhibited the LPS-induced increase in the transvascular permeability of albumin in lung microvessels. Next, we investigated the effects of Rab5a depletion on LPS-induced lung injury. Lung injury was analyzed in control and NC siRNA- and Rab5a siRNA-transfected mice challenged with LPS. Histological examination of lung tissues from LPS-treated control mice and NC siRNA-transfected mice revealed pulmonary congestion, edema, alveoli collapse, and enhanced alveolar wall thickening and infiltration of white blood cells into the lung interstitium and alveolar spaces. However, Rab5a siRNA transfection significantly alleviated the LPS-induced lung injury (Fig. 10d). Intriguingly, after transfection of mice with Rab5a siRNA, longer survival was observed in the LPS-induced sepsis model than in the controls ($p < 0.05$, Fig. 10e). These results suggest that silencing Rab5a with siRNA attenuates LPS-induced endothelial barrier dysfunction in vivo.

Discussion

In this study, we demonstrate that the expression of Rab5a is enhanced by the inflammation mediator LPS, which causes VE-cadherin internalization and actin cytoskeleton remodeling. Suppression of Rab5a expression can maintain endothelial apical–basal cell polarity by inhibiting VE-cadherin internalization, thereby preventing LPS-induced endothelial barrier dysfunction.

Overexpression of Rab5a in HPMECs after LPS treatment in vitro and in vivo

In this report, we demonstrate that the expression of active and total Rab5a is up-regulated after LPS challenge in HPMECs. Moreover, the expression of Rab5a was found to be elevated in the lung endothelium in a sepsis model (Fig. 9). These data suggest that Rab5a may be critical in the regulation of LPS-induced endothelial barrier dysfunction.

Endothelial barrier function is regulated at the level of junctional proteins, which are connected to the actin cytoskeleton via protein complexes [5, 33]. There are many mechanisms that regulate VE-cadherin, such as regulating VE-cadherin activity through phosphorylation and managing the amount of VE-cadherin localized at the cell surface [34–37]. It has been shown that p120-catenin and β-arrestin can directly associate with VE-cadherin and regulate endothelial barrier function. The interaction of p120-catenin and VE-cadherin prevents the clathrin-dependent endocytosis of VE-cadherin and maintains endothelial barrier function, while β-arrestin promotes the internalization of VE-cadherin into clathrin-coated vesicles [35, 36, 38]. In this report, we confirm that LPS induces VE-cadherin internalization and reduces the amount of VE-cadherin expression at the plasma membrane [39]. In agreement with previous studies [39–41], we also observed that LPS induced actin cytoskeleton reorganization in HPMECs, causing stress fiber and intracellular gap formation and disrupting endothelial barrier function (Fig. 2). It has been shown that promoting the clathrin-dependent endocytosis of VE-cadherin reduces the available amount of VE-cadherin in the plasma membrane and disrupts endothelial barrier function. As an early endosome marker, Rab5a plays a crucial role in clathrin-dependent endocytosis.

Therefore, the mechanism of LPS-induced VE-cadherin internalization may be related to the enhanced expression of Rab5a.

Rab5 regulates VE-cadherin localization and F-actin organization in HPMECs

As discussed above, Rab5a is up-regulated during LPS-induced endothelial barrier disruption. We also found that in the absence of Rab5a, the internalization of VE-cadherin induced by LPS was significantly reduced, as were intercellular gaps. Inhibition of Rab5a also prevented F-actin rearrangement and inhibited stress fiber formation. These results were consistent with the protective effect of Rab5a siRNA against endothelial barrier injury.

Prior to this study, Rab5a was mainly known to regulate the clathrin-dependent internalization of multiple cell surface receptors, such as G protein-coupled receptors [25, 26, 42, 43]. Rab5a was also shown to be involved in cell junction protein endocytosis and recycling. In epithelial cells, calcium depletion leads to a rapid clathrin-dependent internalization of several junctional molecules, including JAM-A, occludin, ZO-1, E-cadherin, and β-catenin, and these internalized junctional markers colocalize with Rab5a [44]. Coyne et al. [29] reported that Rab5a and Rab34 participate in Coxsackie virus invasion by regulating the internalization of occludin in Caco-2 cells. In endothelial cells, Rab5a also regulates the redistribution of JAM-A and claudin-1 localization [27, 28]. It has been reported that Rab5 participates in actin remodeling induced by receptor tyrosine kinases (RTKs) [45]. On the other hand, Andrea Palamidessi et al. [30] have shown that Rab5 activates Rac and actin dynamics. Several studies have found that active Rac in endothelial cells can cause vascular hyperpermeability, and Rac has been shown to be involved in TNF-α- and VEGF-induced increases in vascular permeability [46–49]. In addition, LPS can induce the activation of Rac in the lungs in vivo, and inhibiting the activation of Rac with the Rac inhibitor NSC23766 alleviates LPS-induced lung injury [50]. Therefore, the mechanism through which Rab5a regulates VE-cadherin localization and actin cytoskeleton organization as demonstrated in this study may involve Rac activation and the subsequent induction of junctional disassembly and cytoskeleton remodeling.

Rab5a regulates cell polarity and endothelial barrier function in HPMECs

The mechanisms underlying cell polarity in epithelial cells have been well established and a number of proteins are involved in the maintenance of epithelial apical–basal polarity [19, 51–54]. However, similar investigations have only recently elucidated the molecules controlling endothelial cell polarity. VE-cadherin, cerebral cavernous malformation protein 1 (CCM1), and β1 integrin can regulate endothelial cell polarity via a PAR3-dependent mechanism [6, 55]. Moreover, PAR3 can interact with VE-cadherin, JAM-2, and JAM-3 to regulate tight junction stability and endothelial barrier integrity [14, 16, 17, 56]. In addition, the arrangement of the actin cytoskeleton might be implicated in cell polarity [57]. Whitehead et al. [58] reported that CCM2 can limit Rho activation and thereby reduce endothelial cell contractility and vascular permeability. It is possible that CCM2 may also contribute indirectly to the establishment of cell polarity by reshaping the cytoskeleton. All of these findings demonstrate the close relationship between cell polarity and endothelial permeability.

In the present study, we have demonstrated that Rab5a is implicated as a crucial regulator of cell polarity and vascular permeability. We initially found that LPS induced VE-cadherin internalization, resulting in the disruption of apical–basal cell polarity and endothelial barrier dysfunction (Figs. 2, 3, 7). Because knocking down Rab5a expression was able to attenuate LPS-induced VE-cadherin internalization and F-actin remodeling, we investigated whether Rab5a modulated the LPS-induced disruption of cell polarity as well. Our results demonstrated that knocking down Rab5a expression reversed the LPS-induced abnormal cell polarity. It has been shown that Rac1 and Cdc42 regulate cell polarity [59]. As discussed above, Rab5 can induce Rac activation [30]. Therefore, the inflammatory mediator LPS may activate the Rab5a–Rac–VE-cadherin signaling pathway to disrupt endothelial cell polarity and barrier function.

Inhibition of Rab5a overexpression prevents LPS-induced lung injury

Our in vitro experiments have demonstrated the critical role of Rab5a in LPS-induced barrier dysfunction. Consistent with our in vitro results, Rab5a depletion was found to accelerate LPS-induced lung microvascular permeability and inflammation (Fig. 10). However, previous studies have mainly focused on changes in the active GTP-bound form of Rab5a after stimulation. In our work, we observed that the expression of active and total Rab5a was up-regulated after LPS challenge, and the depletion of Rab5a prevented LPS-induced endothelial barrier function and lung injury. These results are consistent with the findings of Wang et al. [60] who reported that Rab10 expression was increased upon LPS stimulation in both dendritic cells and macrophages, and overexpression of Rab10 in macrophages enhanced LPS-induced acute lung injury. Collectively, these results demonstrate that Rab5a is critical for LPS-induced endothelial hyperpermeability. Because in addition to endothelial cells Rab5a siRNA transfection in vivo may also reduce Rab5a expression in other cells, the mechanisms by which Rab5a regulates endothelial barrier function in vivo needs further investigation.

Conclusion

Our studies have provided strong evidence showing that Rab5a is involved in the regulation of LPS-induced endothelial barrier dysfunction. This function of Rab5 is likely mediated through enhancing the internalization of VE-cadherin and the reorganization of the actin cytoskeleton, which subsequently lead to abnormal cell polarity and the disruption of the endothelial barrier. These studies suggest that Rab5a may be a potential therapeutic target for preventing endothelial barrier disruption and vascular inflammation.

Supplementary Material

Refer to Web version on PubMed Central for supplementary material.

Acknowledgments

This research was supported by NSFC grant No. 81170066 and 81370168, and 81201498; and NIH GM076167.

Abbreviations

HPMECs	Human pulmonary microvascular endothelial cells
LPS	Lipopolysaccharide
VE-cadherin	Vascular endothelial-cadherin
Rab5a WT	Wild-type Rab5a
siRNA	Small interference RNA
ALI	Acute lung injury
ARDS	Acute respiratory distress syndrome
BSA	Bovine serum albumin
CI	Cell index
VEGF	Vascular endothelial growth factor
JAM-A	Junction adhesion molecule A
PAR3	Partitioning defective 3
PAR6	Partitioning defective 6
aPKC	Atypical protein kinase C
PCP	Planar cell polarity
Podxl	Podocalyxin
F-actin	Filamentous actin
EBA	Evans blue albumin
WB	Western blot
i.p.	Intraperitoneal

References

1. Mehta D, Malik AB. Signaling mechanisms regulating endothelial permeability. Physiol Rev. 2006; 86:279–367. [PubMed: 16371600]
2. Komarova YA, Mehta D, Malik AB. Dual regulation of endothelial junctional permeability. Sci STKE. 2007; 2007:e8.
3. Harris ES, Nelson WJ. VE-cadherin: at the front, center, and sides of endothelial cell organization and function. Curr Opin in Cell Biol. 2010; 22:651–658. [PubMed: 20708398]
4. Giannotta M, Trani M, Dejana E. VE-cadherin and endothelial adherens junctions: active guardians of vascular integrity. Dev Cell. 2013; 26:441–454. [PubMed: 24044891]
5. Komarova Y, Malik AB. Regulation of endothelial permeability via paracellular and transcellular transport pathways. Annu Rev Physiol. 2010; 72:463–493. [PubMed: 20148685]
6. Lampugnani MG, Orsenigo F, Rudini N, Maddaluno L, Boulday G, Chapon F, Dejana E. CCM1 regulates vascular-lumen organization by inducing endothelial polarity. J Cell Sci. 2010; 123:1073–1080. [PubMed: 20332120]
7. Taddei A, Giampietro C, Conti A, Orsenigo F, Breviario F, Pirazzoli V, Potente M, Daly C, Dimmeler S, Dejana E. Endothelial adherens junctions control tight junctions by VE-cadherin-mediated upregulation of claudin-5. Nat Cell Biol. 2008; 10:923–934. [PubMed: 18604199]

8. McCaffrey LM, Macara IG. Widely conserved signaling pathways in the establishment of cell polarity. Cold Spring Harb Perspect Biol. 2009; 1:a1370.
9. Nelson WJ. Remodeling epithelial cell organization: transitions between front–rear and apical–basal polarity. Cold Spring Harb Perspect Biol. 2009; 1:a513.
10. Chen J, Zhang M. The Par3/Par6/aPKC complex and epithelial cell polarity. Exp Cell Res. 2013; 319:1357–1364. [PubMed: 23535009]
11. Suzuki A, Ohno S. The PAR-aPKC system: lessons in polarity. J Cell Sci. 2006; 119:979–987. [PubMed: 16525119]
12. Martin-Belmonte F, Mostov K. Regulation of cell polarity during epithelial morphogenesis. Curr Opin Cell Biol. 2008; 20:227–234. [PubMed: 18282696]
13. Macara IG. Parsing the polarity code. Nat Rev Mol Cell Biol. 2004; 5:220–231. [PubMed: 14991002]
14. Iden S, Rehder D, August B, Suzuki A, Wolburg-Buchholz K, Wolburg H, Ohno S, Behrens J, Vestweber D, Ebnet K. A distinct PAR complex associates physically with VE-cadherin in vertebrate endothelial cells. EMBO Rep. 2006; 7:1239–1246. [PubMed: 17057644]
15. Daneman R, Zhou L, Agalliu D, Cahoy JD, Kaushal A, Barres BA. The mouse blood-brain barrier transcriptome: a new resource for understanding the development and function of brain endothelial cells. PLoS One. 2010; 5:e13741. [PubMed: 21060791]
16. Artus CD, Glacial F, Ganeshamoorthy K, Ziegler N, Godet M, Guilbert T, Liebner S, Couraud P. The Wnt/planar cell polarity signaling pathway contributes to the integrity of tight junctions in brain endothelial cells. J Cereb Blood Flow Metab. 2013; 34:433–440. [PubMed: 24346691]
17. Tyler RC, Peterson FC, Volkman BF. Distal interactions within the par3-VE-cadherin complex. Biochemistry. 2010; 49:951–957. [PubMed: 20047332]
18. Grosshans BL, Ortiz D, Novick P. Rabs and their effectors: achieving specificity in membrane traffic. Proc Natl Acad Sci USA. 2006; 103:11821–11827. [PubMed: 16882731]
19. Zerial M, McBride H. Rab proteins as membrane organizers. Nat Rev Mol Cell Biol. 2001; 2:107–117. [PubMed: 11252952]
20. Bucci C, Lutcke A, Steele-Mortimer O, Olkkonen VM, Dupree P, Chiariello M, Bruni CB, Simons K, Zerial M. Co-operative regulation of endocytosis by three Rab5 isoforms. FEBS Lett. 1995; 366:65–71. [PubMed: 7789520]
21. Torres VA, Stupack DG. Rab5 in the regulation of cell motility and invasion. Curr Protein Pept Sci. 2011; 12:43–51. [PubMed: 21190523]
22. Lanzetti L. A novel function of Rab5 in mitosis. Small GTPases. 2012; 3:168–172. [PubMed: 22694819]
23. Mendoza P, Ortiz R, Diaz J, Quest AFG, Leyton L, Stupack D, Torres VA. Rab5 activation promotes focal adhesion disassembly, migration and invasiveness in tumor cells. J Cell Sci. 2013; 126:3835–3847. [PubMed: 23813952]
24. Li Y, Zhao Y, Hu J, Xiao J, Qu L, Wang Z, Ma D, Chen Y. A novel ER-localized transmembrane protein, EMC6, interacts with RAB5A and regulates cell autophagy. Autophagy. 2014; 9:150–163. [PubMed: 23182941]
25. Seachrist JL, Anborgh PH, Ferguson SS. Beta 2-adrenergic receptor internalization, endosomal sorting, and plasma membrane recycling are regulated by rab GTPases. J Biol Chem. 2000; 275:27221–27228. [PubMed: 10854436]
26. Seachrist JL, Ferguson SSG. Regulation of G protein-coupled receptor endocytosis and trafficking by Rab GTPases. Life Sci. 2003; 74:225–235. [PubMed: 14607250]
27. Stamatovic SM, Sladojevic N, Keep RF, Andjelkovic AV. Relocalization of junctional adhesion molecule a during inflammatory stimulation of brain endothelial cells. Mol Cell Biol. 2012; 32:3414–3427. [PubMed: 22733993]
28. Asaka M, Hirase T, Hashimoto-Komatsu A, Node K. Rab5a-mediated localization of claudin-1 is regulated by proteasomes in endothelial cells. AJP: cell. Physiology. 2010; 300:C87–C96. [PubMed: 20926780]
29. Coyne CB, Shen L, Turner JR, Bergelson JM. Coxsackievirus entry across epithelial tight junctions requires occludin and the small GTPases Rab34 and Rab5. Cell Host Microbe. 2007; 2:181–192. [PubMed: 18005733]

30. Palamidessi A, Frittoli E, Garre M, Faretta M, Mione M, Testa I, Diaspro A, Lanzetti L, Scita G, Di Fiore PP. Endocytic trafficking of Rac is required for the spatial restriction of signaling in cell migration. Cell. 2008; 134:135–147. [PubMed: 18614017]
31. Li Y, Wang G, Lin K, Yin H, Zhou C, Liu T, Wu G, Qian G. Rabl GTPase promotes expression of β-adrenergic receptors in rat pulmonary microvascular endothelial cells. Int J Biochem Cell Biol. 2010; 42:1201–1209. [PubMed: 20417717]
32. Birukova AA, Fu P, Xing J, Cokic I, Birukov KG. Lung endothelial barrier protection by iloprost in the 2-hit models of ventilator-induced lung injury (VILI) involves inhibition of Rho signaling. Transl Res. 2010; 155:44–54. [PubMed: 20004361]
33. Dejana E. Endothelial cell-cell junctions: happy together. Nat Rev Mol Cell Biol. 2004; 5:261–270. [PubMed: 15071551]
34. Dejana E, Orsenigo F, Lampugnani MG. The role of adherens junctions and VE-cadherin in the control of vascular permeability. J Cell Sci. 2008; 121:2115–2122. [PubMed: 18565824]
35. Xiao K, Garner J, Buckley KM, Vincent PA, Chiasson CM, Dejana E, Faundez V, Kowalczyk AP. p120-Catenin regulates clathrin-dependent endocytosis of VE-cadherin. Mol Biol Cell. 2005; 16:5141–5151. [PubMed: 16120645]
36. Regan-Klapisz E, Krouwer V, Langelaar-Makkinje M, Nallan L, Gelb M, Gerritsen H, Verkleij AJ, Post JA. Golgi-associated cPLA2alpha regulates endothelial cell-cell junction integrity by controlling the trafficking of transmembrane junction proteins. Mol Biol Cell. 2009; 20:4225–4234. [PubMed: 19675210]
37. Xiao K, Allison DF, Buckley KM, Kottke MD, Vincent PA, Faundez V, Kowalczyk AP. Cellular levels of p120 catenin function as a set point for cadherin expression levels in microvascular endothelial cells. J Cell Biol. 2003; 163:535–545. [PubMed: 14610056]
38. Gavard J, Gutkind JS. VEGF controls endothelial-cell permeability by promoting the β-arrestin-dependent endocytosis of VE-cadherin. Nat Cell Biol. 2006; 8:1223–1234. [PubMed: 17060906]
39. Gong H, Gao X, Feng S, Siddiqui MR, Garcia A, Bonini MG, Komarova Y, Vogel SM, Mehta D, Malik AB. Evidence of a common mechanism of disassembly of adherens junctions through Gα13 targeting of VE-cadherin. J Exp Med. 2014; 211:579–591. [PubMed: 24590762]
40. Bogatcheva NV, Zemskova MA, Kovalenkov Y, Poirier C, Verin AD. Molecular mechanisms mediating protective effect of cAMP on lipopolysaccharide (LPS)-induced human lung microvascular endothelial cells (HLMVEC) hyperpermeability. J Cellular Physiol. 2009; 221:750–759. [PubMed: 19725051]
41. Schlegel N, Baumer Y, Drenckhahn D, Waschke J. Lipopolysaccharide-induced endothelial barrier breakdown is cyclic adenosine monophosphate dependent in vivo and in vitro*. Crit Care Med. 2009; 37:1735–1743. [PubMed: 19325485]
42. Jiang X, Pan H, Nabhan JF, Krishnan R, Koziol-White C, Panettieri RA, Lu Q. A novel EST-derived RNAi screen reveals a critical role for farnesyl diphosphate synthase in β2-adrenergic receptor internalization and down-regulation. FASEB J. 2012; 26:1995–2007. [PubMed: 22278941]
43. Jopling HM, Odell AF, Hooper NM, Zachary IC, Walker JH, Ponnambalam S. Rab GTPase regulation of VEGFR2 trafficking and signaling in endothelial cells. Arterioscler Thromb Vasc Biol. 2009; 29:1119–1124. [PubMed: 19372461]
44. Ivanov AI, Nusrat A, Parkos CA. Endocytosis of epithelial apical junctional proteins by a clathrin-mediated pathway into a unique storage compartment. Mol Biol Cell. 2004; 15:176–188. [PubMed: 14528017]
45. Lanzetti L, Palamidessi A, Areces L, Scita G, Di Fiore PP. Rab5 is a signalling GTPase involved in actin remodelling by receptor tyrosine kinases. Nature. 2004; 429:309–314. [PubMed: 15152255]
46. Monaghan-Benson E, Burridge K. The regulation of vascular endothelial growth factor-induced microvascular permeability requires Rac and reactive oxygen species. J Biol Chem. 2009; 284:25602–25611. [PubMed: 19633358]
47. Cain RJ, Vanhaesebroeck B, Ridley AJ. The PI3 K p110α isoform regulates endothelial adherens junctions via Pyk2 and Racl. J Cell Biol. 2010; 188:863–876. [PubMed: 20308428]

48. van Wetering S, van Buul JD, Quik S, Mul FP, Anthony EC, Ten KJ, Collard JG, Hordijk PL. Reactive oxygen species mediate Rac-induced loss of cell-cell adhesion in primary human endothelial cells. J Cell Sci. 2002; 115:1837–1846. [PubMed: 11956315]

49. Naikawadi RP, Cheng N, Vogel SM, Qian F, Wu D, Malik AB, Ye RD. A critical role for phosphatidylinositol (3,4,5)-trisphosphate-dependent rac exchanger 1 in endothelial junction disruption and vascular hyperpermeability. Circ Res. 2012; 111:1517–1527. [PubMed: 22965143]

50. Yao HY, Chen L, Xu C, Wang J, Chen J, Xie QM, Wu X, Yan XF. Inhibition of Rac activity alleviates lipopolysaccharide-induced acute pulmonary injury in mice. Biochim Biophys Acta. 2011; 1810:666–674. [PubMed: 21511011]

51. Sato T, Mushiake S, Kato Y, Sato K, Sato M, Takeda N, Ozono K, Miki K, Kubo Y, Tsuji A, Harada R, Harada A. The Rab8 GTPase regulates apical protein localization in intestinal cells. Nature. 2007; 448:366–369. [PubMed: 17597763]

52. Matter K, Mellman I. Mechanisms of cell polarity: sorting and transport in epithelial cells. Curr Opin Cell Biol. 1994; 6:545–554. [PubMed: 7986532]

53. Rodriguez-Boulan E, Musch A, Le Bivic A. Epithelial trafficking: new routes to familiar places. Curr Opin Cell Biol. 2004; 16:436–442. [PubMed: 15261677]

54. Nelson WJ. Adaptation of core mechanisms to generate cell polarity. Nature. 2003; 422:766–774. [PubMed: 12700771]

55. Zovein AC, Luque A, Turlo KA, Hofmann JJ, Yee KM, Becker MS, Fassler R, Mellman I, Lane TF, Iruela-Arispe ML. β1 integrin establishes endothelial cell polarity and arteriolar lumen formation via a Par3-dependent mechanism. Dev Cell. 2010; 18:39–51. [PubMed: 20152176]

56. Ebnet K, Aurrand-Lions M, Kuhn A, Kiefer F, Butz S, Zander K, Meyer ZB, Suzuki A, Imhof BA, Vestweber D. The junctional adhesion molecule (JAM) family members JAM-2 and JAM-3 associate with the cell polarity protein PAR-3: a possible role for JAMs in endothelial cell polarity. J Cell Sci. 2003; 116:3879–3891. [PubMed: 12953056]

57. Iden S, Collard JG. Crosstalk between small GTPases and polarity proteins in cell polarization. Nat Rev Mol Cell Biol. 2008; 9:846–859. [PubMed: 18946474]

58. Whitehead KJ, Chan AC, Navankasattusas S, Koh W, London NR, Ling J, Mayo AH, Drakos SG, Jones CA, Zhu W, Marchuk DA, Davis GE, Li DY. The cerebral cavernous malformation signaling pathway promotes vascular integrity via Rho GTPases. Nat Med. 2009; 15:177–184. [PubMed: 19151728]

59. Koh W, Mahan RD, Davis GE. Cdc42- and Rac1-mediated endothelial lumen formation requires Pak2, Pak4 and Par3, and PKC-dependent signaling. J Cell Sci. 2008; 121:989–1001. [PubMed: 18319301]

60. Wang D, Lou J, Ouyang C, Chen W, Liu Y, Liu X, Cao X, Wang J, Lu L. Ras-related protein Rab10 facilitates TLR4 signaling by promoting replenishment of TLR4 onto the plasma membrane. Proc Natl Acad Sci USA. 2010; 107:13806–13811. [PubMed: 20643919]

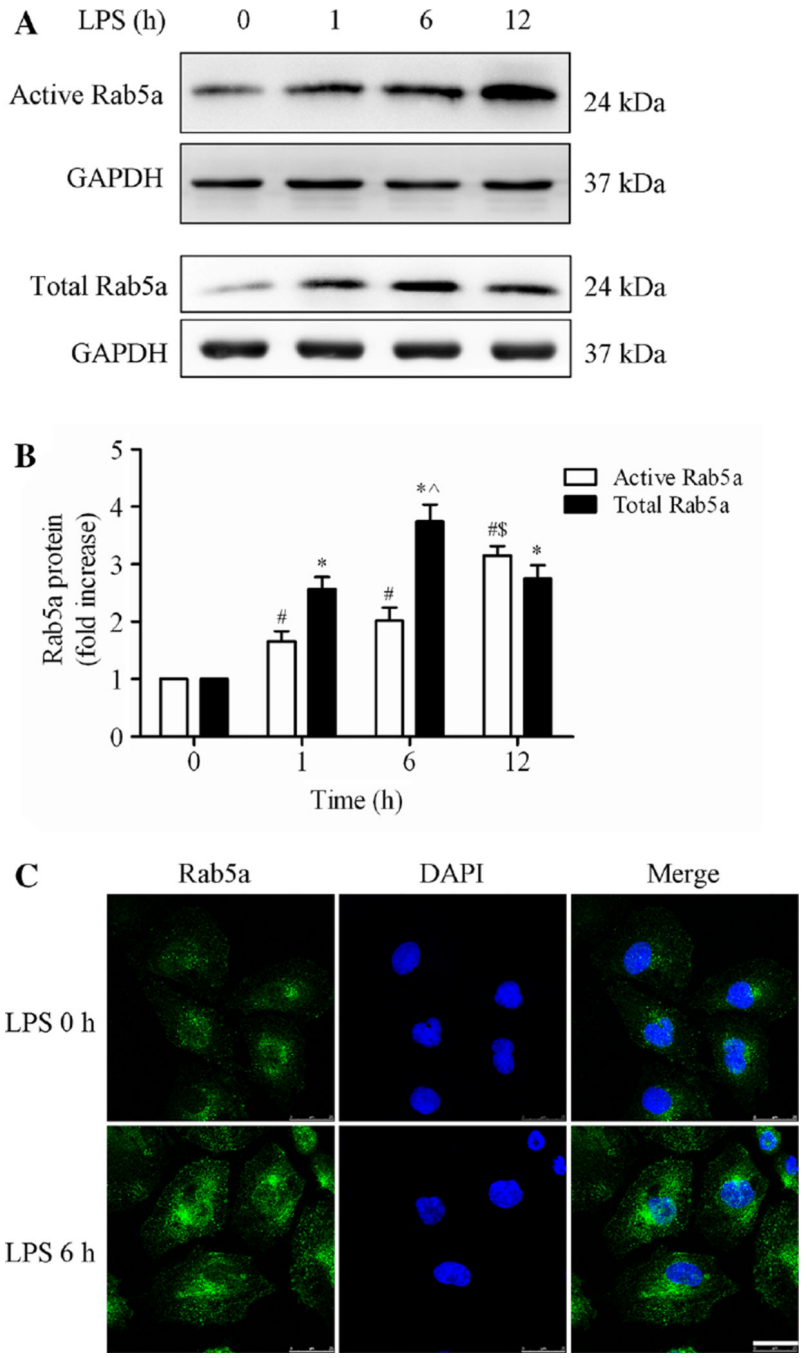

Fig. 1. Effect of LPS on the activity and expression of Rab5a in HPMECs

a Expression of active and total Rab5a was measured by pulldown assay and Western blotting (WB) using polyclonal antibodies against Rab5a. *Representative blots* showing active Rab5a (*upper panel*), relative GAPDH (*2nd panel*), total Rab5a (*3rd panel*), and GAPDH expression (*lower panel*) are shown. HPMECs were cultured and treated with LPS (1 μg/ml) for various time intervals (1, 6, and 12 h). **b** Quantitative data of active and total Rab5a expression normalized to GAPDH expression. The data are presented as the mean ± SE ($n = 3$). For active Rab5a, $^{\#}p < 0.05$ versus the 0 h group, $^{\$}p < 0.05$ versus the 1 h group;

for total Rab5a, *$p < 0.05$ versus the 0 h group, ^$p < 0.05$ versus the 1 h group. **c** HPMECs were cultured on coverslips and then treated with 1 μg/ml LPS for 6 h, fixed, and stained with an anti-Rab5a polyclonal antibody. The *images* represent three separate experiments. *Green*, Rab5a; *blue*, DNA stained with DAPI (nuclei). *Scale bar*, 25 μm

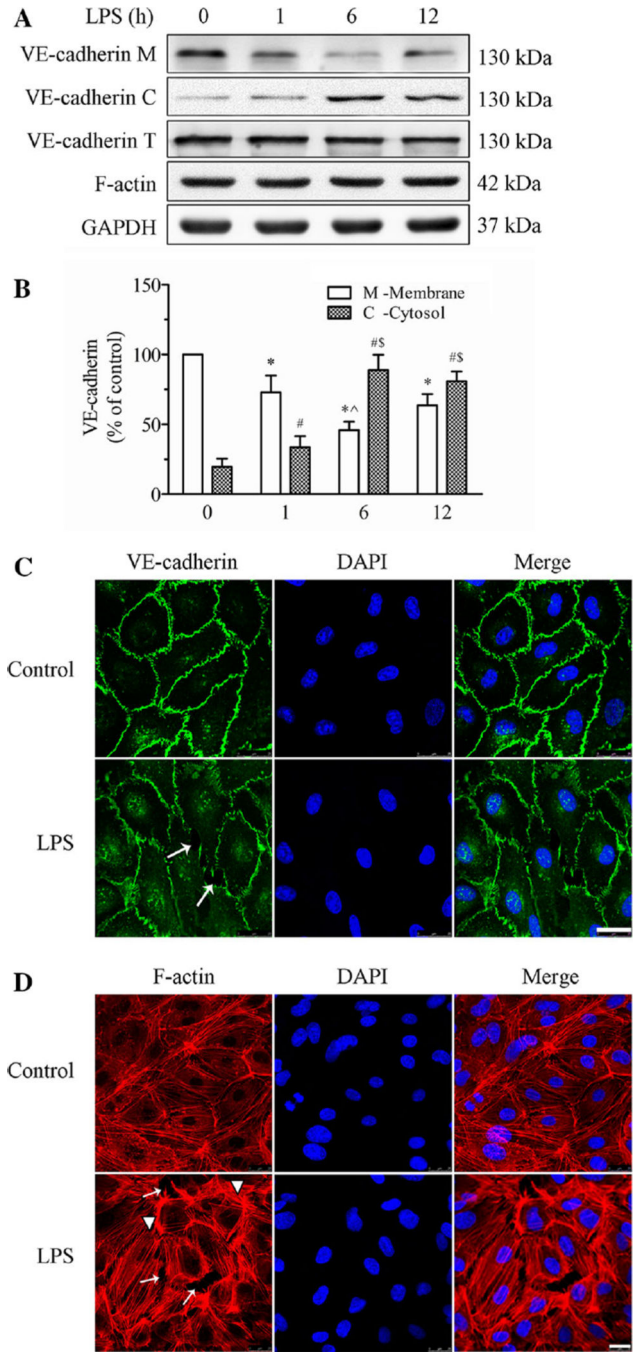

Fig. 2. Effect of LPS on the expression and localization of VE-cadherin and the actin cytoskeleton in HPMECs

a The expression levels of the VE-cadherin and F-actin in the membrane and cytosol fractions and whole cell lysate were detected by WB. *Representative blots* showing the expression of VE-cadherin in the cell membrane (*upper panel*), in the cytosol (*2nd panel*), and in the whole cells (*3rd panel*), and the expressions of F-actin (*4th panel*) and GAPDH (*lower panel*) are shown. HPMECs were treated with 1 μg/ml LPS for various time intervals. **b** Histogram showing the quantification of VE-cadherin in the membrane fraction (*white*

bars) and in the cytosol fraction (*grid bars*) from three independent experiments. The data are presented as the mean ± SE $*p < 0.05$ versus the 0 h membrane group, $^{\wedge}p < 0.05$ versus the 1 h membrane group; $^{\#}p < 0.05$ versus the 0 h cytosolic group, $^{\$}p < 0.05$ versus the 1 h cytosolic group. **c, d** Confocal microscopic analysis of VE-cadherin (**c**) and F-actin (**d**) in HPMECs after LPS treatment. HPMECs were cultured on Transwell inserts for 5–7 days. The HPMECs were grown to about 90 % confluence. They were stimulated with 1 μg/ml LPS for 6 h and imaged by confocal laser scanning microscopy (CLSM). *Green* indicates cells labeled with VE-cadherin; *red*, F-actin; *blue*, DAPI. *Arrows* indicate intercellular gaps and *arrowheads* indicate fibers. *Scale bar* 25 μm. The *photographs* represent three separate experiments

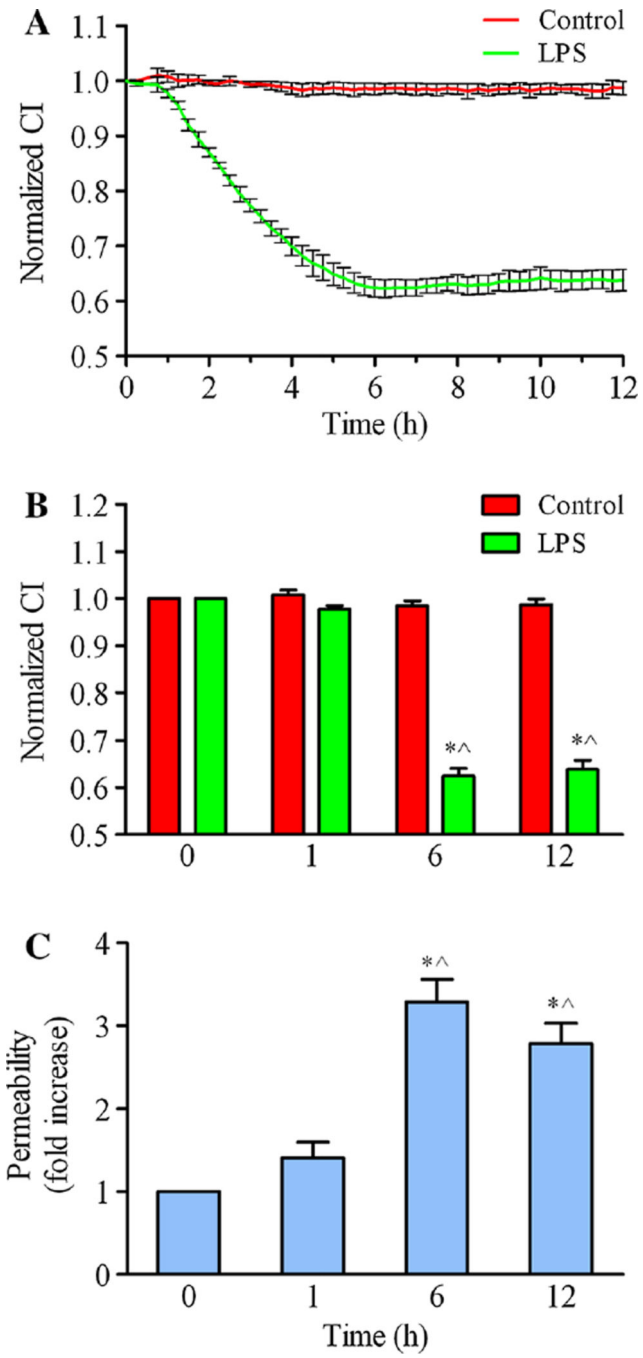

Fig. 3. HPMEC barrier dysfunction after LPS treatment

a HPMECs were cultured and stimulated with LPS at 1 μg/ml, and real-time cell growth curves were subsequently observed and taken from four independent experiments using the iCELLigence system. **b** A time histogram shows the normalized cell index (CI) with LPS treatment for 1, 6, and 12 h. The data are presented as the mean ± SE. $n = 4$, $^{*}p < 0.05$ versus the 0 h group, $^{\wedge}p < 0.05$ versus the 1 h group. **c** HPMECs were grown to confluence on 0.4-μm Transwell inserts and stimulated with 1 μg/ml LPS for different time intervals (1,6, and 12 h). FITC-dextran was added to the upper wells at a concentration of 1 mg/mL.

After 0.5 h of incubation, 50 μl of medium from the bottom chamber was aspirated and measured in a fluorescence plate reader. The FITC-dextran permeability is expressed as the fold increase ±SE ($n = 3$). *$p < 0.05$ versus the 0 h group, ^$p < 0.05$ versus the 1 h group

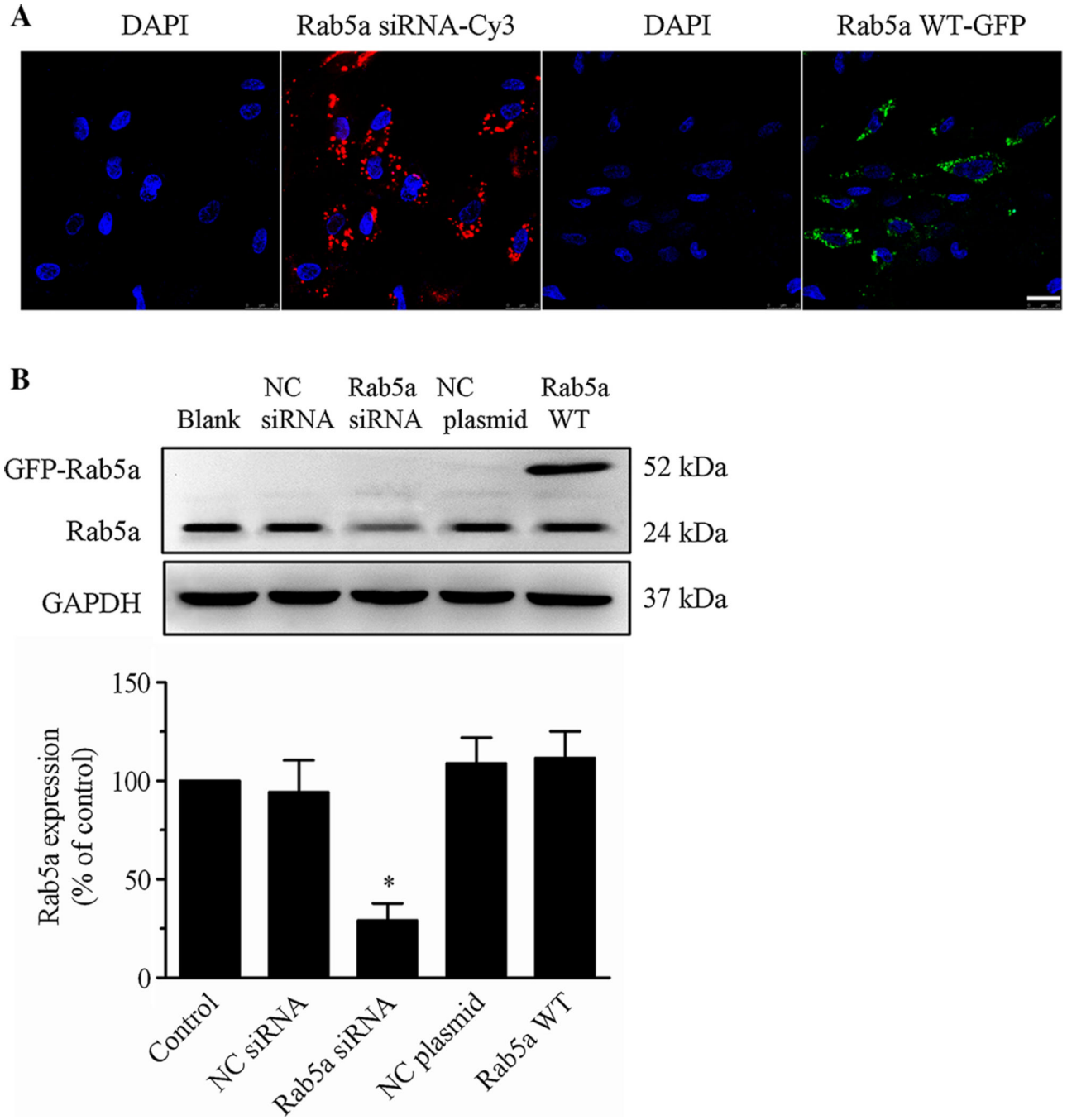

Fig. 4. Transfection of Rab5a siRNA and the WT Rab5a plasmid into HPMECs

a Efficiency of Rab5a siRNA and WT Rab5a plasmid transfection in HPMECs. HPMECs were cultured on coverslips and transfected with either Cy3-tagged Rab5a siRNA for 12 h using the X-tremeGENE siRNA Transfection Reagent or the GFP-tagged WT Rab5a plasmid for 48 h using the X-tremeGENE HP DNA Transfection Reagent. The localization of Rab5a siRNA and Rab5a WT in HPMECs was detected using CLSM. Similar results were obtained in three separate experiments. *Blue*, DNA staining with DAPI (nuclear); *red*, Cy3; *green*, GFP. *Scale bar* 25 μm. **b** Rab5a expression in HPMECs after transfection with

Rab5a siRNA was assayed. HPMECs were transfected with NC siRNA (control siRNA), Rab5a siRNA, NC plasmid (empty plasmid), or the Rab5a–GFP WT plasmid. *Representative bands* showing Rab5a (*upper panel*) and GAPDH expression (*lower panel*) are shown. A histogram illustrates the quantitative analysis of the protein levels of endogenous Rab5a, normalized to GAPDH expression. The data are presented as the mean ± SE. $n = 3$. $^{*}p < 0.05$ versus the control and NC siRNA groups

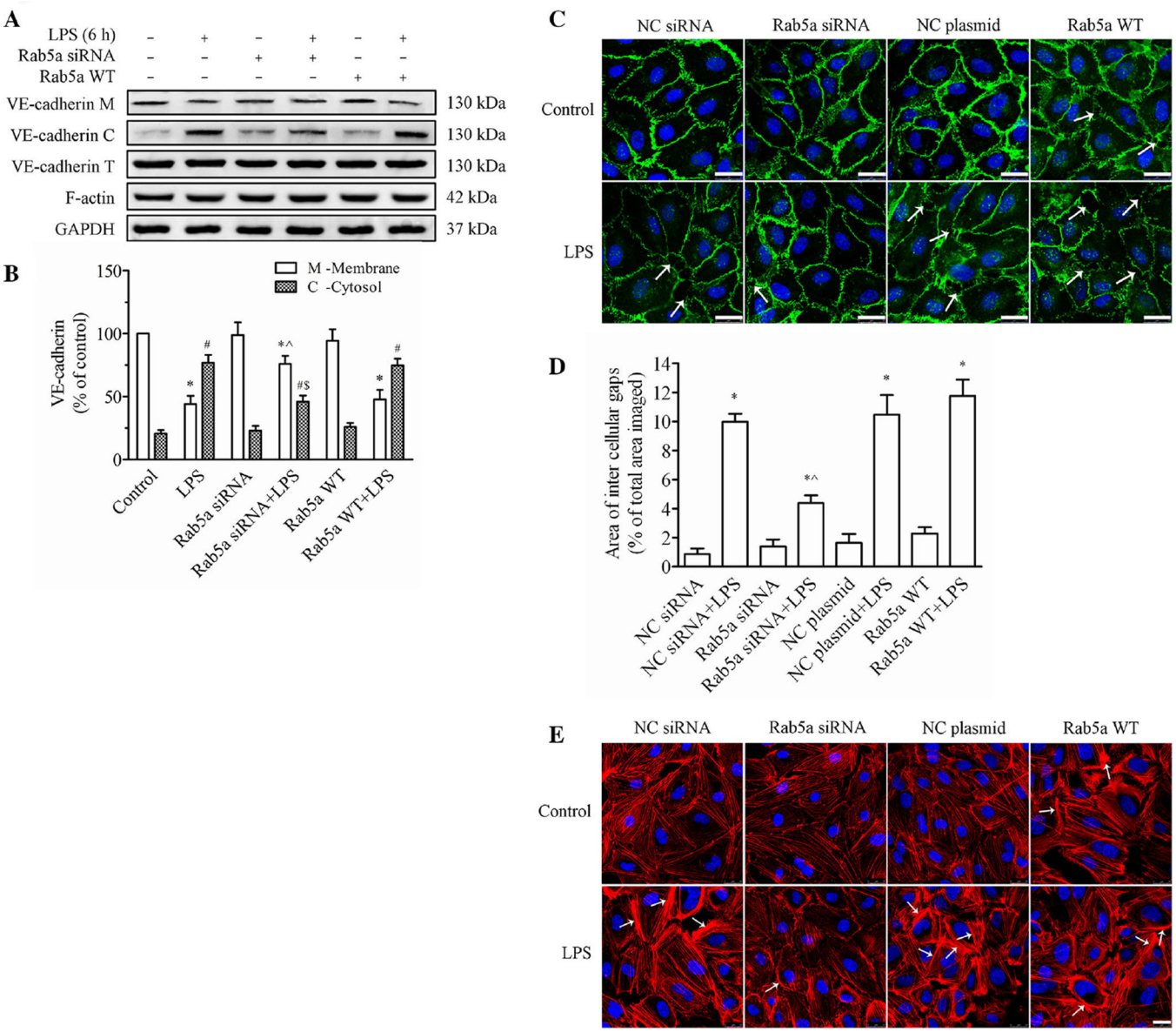

Fig. 5. Rab5a regulates the LPS-induced disruption of VE-cadherin and actin cytoskeleton remodeling in HPMECs

a The expression levels of VE-cadherin and F-actin in the cell membrane, cell cytosol fractions, and whole cells were determined by WB. *Representative blots* showing the expression of VE-cadherin in the membrane (*upper panel*), cytosol (*2nd panel*), and whole cells (*3rd panel*), F-actin (*4th panel*), and GAPDH (*5th panel*) are shown. HPMECs were transfected with or without Rab5a siRNA or the Rab5a WT plasmid and then treated with 1 μg/ml LPS for 6 h. **b** Quantitative data showing VE-cadherin protein levels in the cell membrane and cytosol, normalized to GAPDH expression. The data are presented as the mean ± SE $n = 3$. $^{*}p < 0.05$ versus the membrane control group, $^{\wedge}p < 0.05$ versus the membrane LPS group; $^{\#}p < 0.05$ versus the cytosolic control group, $^{\$}p < 0.05$ versus the cytosolic LPS group. **c** Localization of VE-cadherin in HPMECs following Rab5a siRNA or WT plasmid transfection. After pretransfection with NC siRNA, Rab5a siRNA, the NC

plasmid, or the WT Rab5a plasmid, confluent HPMECs were stimulated with 1 μg/ml LPS for 6 h. VE-cadherin localization was detected by CLSM. *Green*, VE-cadherin; *blue*, DAPI. *Arrows* indicate intercellular gaps. *Scale bar* 25 μm. The *photographs* represent three independent experiments. **d** Quantification of the area of intercellular gaps as a percentage of the total area imaged. The data are presented as the mean ± SE based on three independent experiments. $*p < 0.05$ versus the NC siRNA group, $^{\wedge}p < 0.05$ versus the NC siRNA plus LPS treatment group. **e** Localization of the expression of F-actin in HPMECs following Rab5a siRNA or WT plasmid transfection. After pretransfection with NC siRNA, Rab5a siRNA, the NC plasmid, or the Rab5a WT plasmid, HPMECs were stimulated or not stimulated with 1 μg/ml LPS for 6 h. The actin cytoskeleton was stained with rhodamine-phalloidin and observed via CLSM. *Red*, F-actin; *blue*, DAPI. *Arrows* indicate stress fibers. *Scale bar* 25 μm. The *photographs* represent three independent experiments

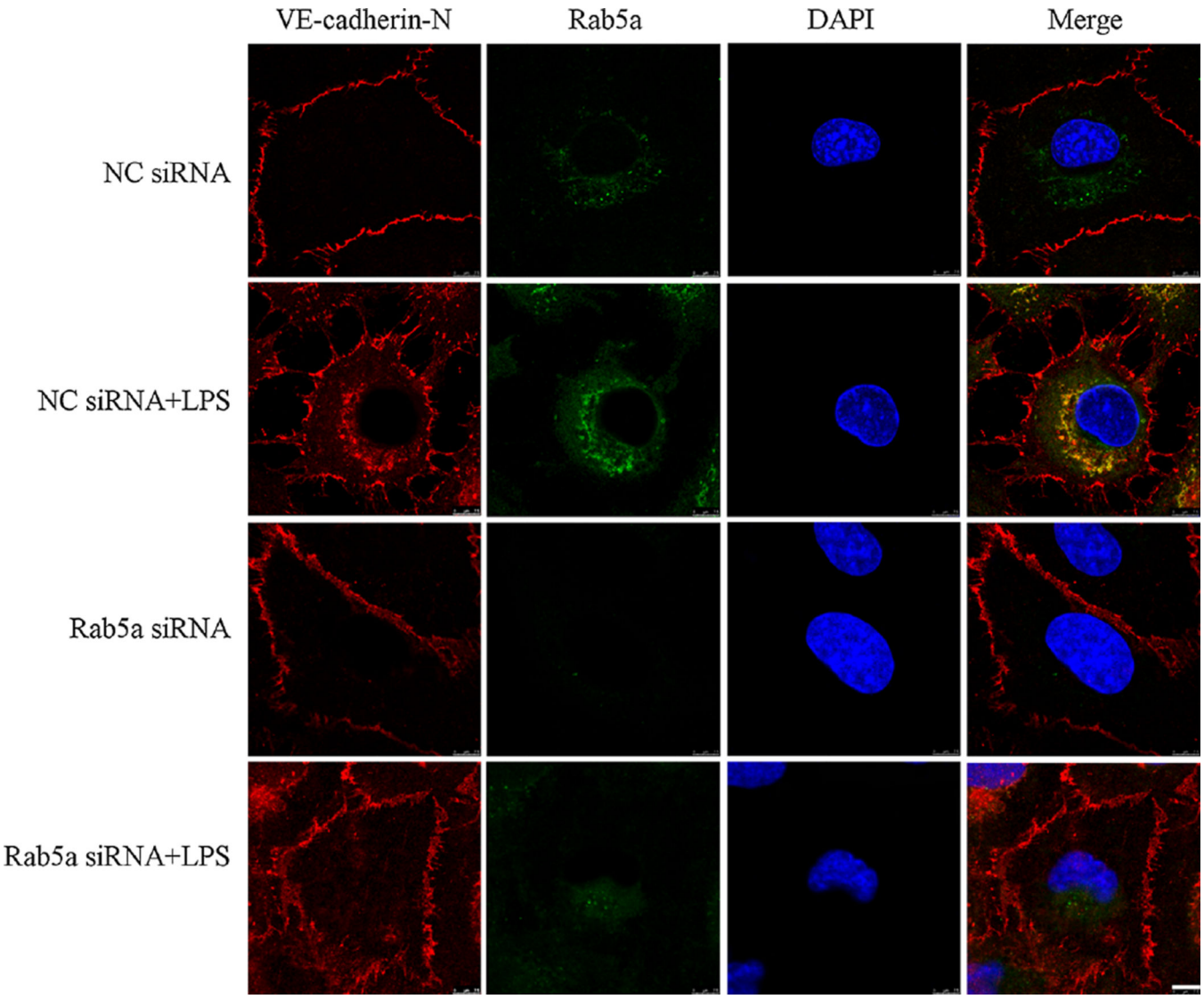

Fig. 6. Knockdown of Rab5a inhibits LPS-induced VE-cadherin internalization in HPMECs

HPMECs were transfected with NC siRNA or Rab5a siRNA and stimulated with 1 μg/ml LPS for 6 h, and then incubated with anti-VE-cadherin antibodies against the extracellular domain of VE-cadherin (VE-cadherin-*N* at 4 °C for 1 h. The VE-cadherin internalization was monitored by the uptake of external VE-cadherin antibodies at 37 °C and visualized in fixed cells using secondary fluorescent antibodies (*red*). The cells were also stained with Rab5a antibodies (*green*). Colocalization between VE-cadherin and Rab5a was displayed as *yellow color* in these overlays. *Scale bar* 7.5 μm. The *photographs* represent three independent experiments

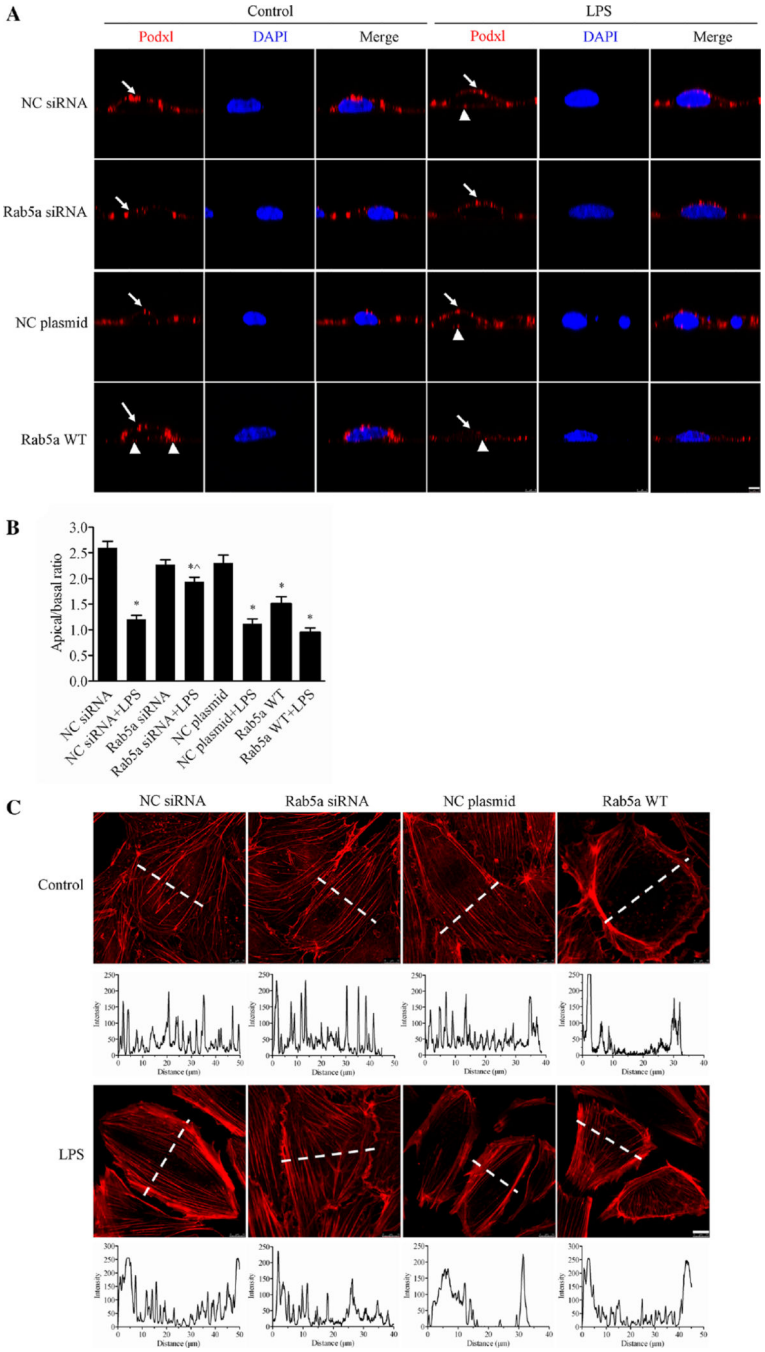

Fig. 7. Rab5a regulates the LPS-induced disruption of human endothelial cell polarity

a Inhibitory effect of Rab5a siRNA on the LPS-induced disruption of HPMEC polarity. HPMECs cultured on Transwell inserts and transfected with NC siRNA, Rab5a siRNA, the NC plasmid, or the WT Rab5a plasmid were treated with 1 μg/ml of LPS for 6 h. The cells were then labeled with the apical protein marker Podxl. *Red*, Podxl; *blue*, DAPI. *Arrows* indicate Podxl localized at the apical surface of the cell. *Arrowheads* indicate Podxl distribution at the basal rather than apical surface of the cell. *Z-axis, scale bar* 5 μm. **b** Quantification of the apical/basal fluorescence intensity of the Podxl protein over time in a

histogram. The apical or basal fluorescence intensity was calculated by integrating the area under the apical or basal peak defined via membrane labeling with Podxl using ImageJ software. The mean apical/basal fluorescence intensity was calculated in ten cells from three independent experiments. *$p < 0.05$ versus the NC siRNA group; ^$p < 0.05$ versus the NC siRNA plus LPS treatment group. **c** Inhibitory effect of Rab5a siRNA on the LPS-induced disruption of the F-actin cytoskeleton. Photograph of red fluorescence showing the distribution of F-actin in HPMECs (*upper panel*). Following pretransfection with NC siRNA, Rab5a siRNA, the NC plasmid, and the WT Rab5a plasmid, confluent HPMECs were stimulated with 1 μg/ml LPS for 6 h. The F-actin cytoskeleton was stained with rhodamine-phalloidin. *Red*, F-actin; *blue*, DAPI. *Scale bar*, 10 μm. Quantification of the F-actin fluorescence intensity is indicated in the corresponding histograms below the fluorescence images, which represent the intensity profiles of F-actin staining along the dotted lines in the photomicrographs, emphasizing differences in the cross-cellular F-actin expression

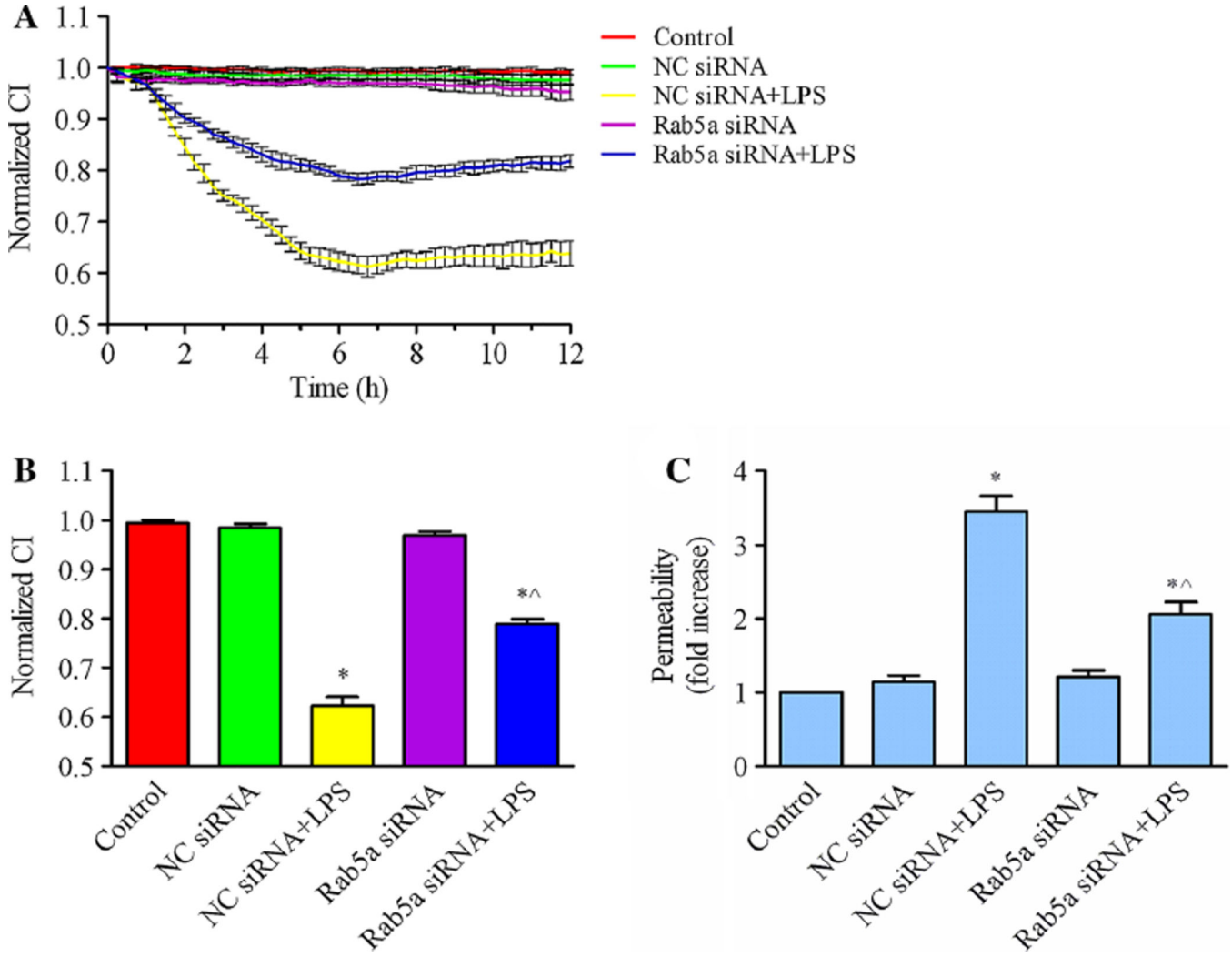

Fig. 8. Rab5a regulates LPS-induced HPMEC dysfunction

a HPMECs were transfected with NC siRNA or Rab5a siRNA for 48 h and then stimulated with 1 μg/ml LPS for 6 h. Real-time cell growth curves were generated using the iCELLigence system. The data are shown as the mean ± SE from three independent experiments. **b** Quantification of the normalized CI in the histogram. After transfection with NC siRNA and Rab5a siRNA, the cells were stimulated with LPS for 6 h. The data are presented as the mean ± SE, $n = 3$. *$p < 0.05$ versus the control group; ^$p < 0.05$ versus the NC siRNA plus LPS treatment group. **c** HPMECs were cultured on 0.4-μm Transwell inserts and transfected with NC siRNA or Rab5a siRNA for 48 h and then stimulated with 1 μg/ml LPS for 6 h. FITC-dextran was added to the upper wells at a concentration of 1 mg/ml. After 0.5 h of incubation, 50 μl of medium from the bottom chamber was aspirated and analyzed using a fluorescence plate reader. FITC-dextran permeability was expressed as fold increase ± SE ($n = 3$). *$p < 0.05$ versus the control group; ^$p < 0.05$ versus the NC siRNA plus LPS treatment group

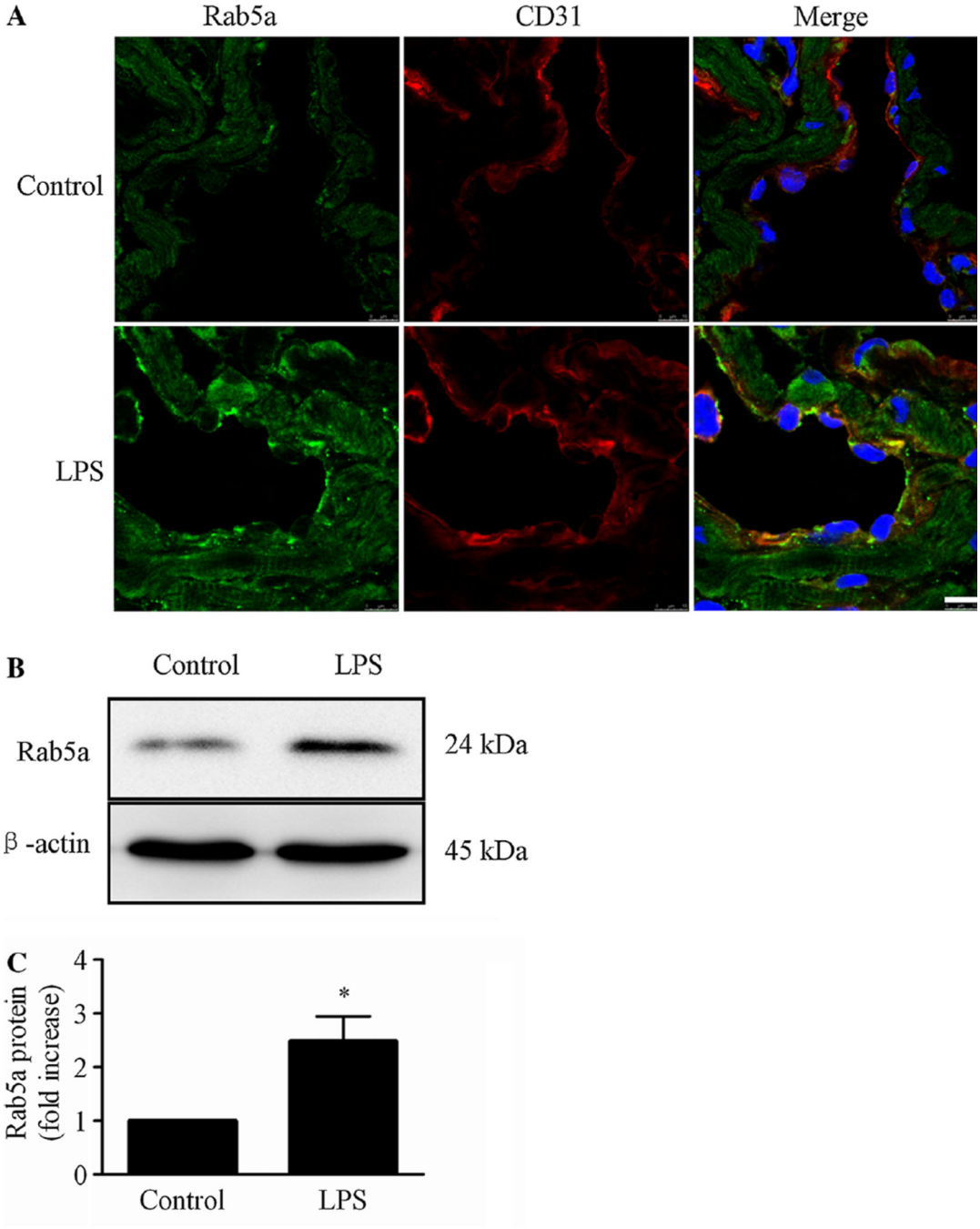

Fig. 9. Rab5a expression is elevated by LPS treatment in mouse lungs in vivo

a C57BL/6 mice received i.p. injections with saline or 20 mg/kg LPS. OTC-embedded lung sections were prepared 24 h after LPS challenge. Rab5a expression in the endothelium was analyzed by CLSM. *Green* indicates labeling of Rab5a; *red*, CD31; *blue*, DAPI. *Scale bar* 7.5 μm. The *figures* represent three experiments. Note: a floating nucleus at the *upper left* of the image in the LPS group is a contaminted white blood cell's nucleus in the vascular lumen. **b** C57BL/6 mice were i.p. injected with saline or 20 mg/kg LPS. Lung tissues were collected after 24 h of treatment. Rab5a expression was analyzed via WB. Representative

blots showing Rab5a (*upper panel*) and β-actin expression (*lower panel*) are shown. *Lower panel* shows quantitative data corresponding to Rab5a protein levels normalized to β-actin expression. The data are presented as the mean ± SE $n = 3$. *$p < 0.05$ versus the control group

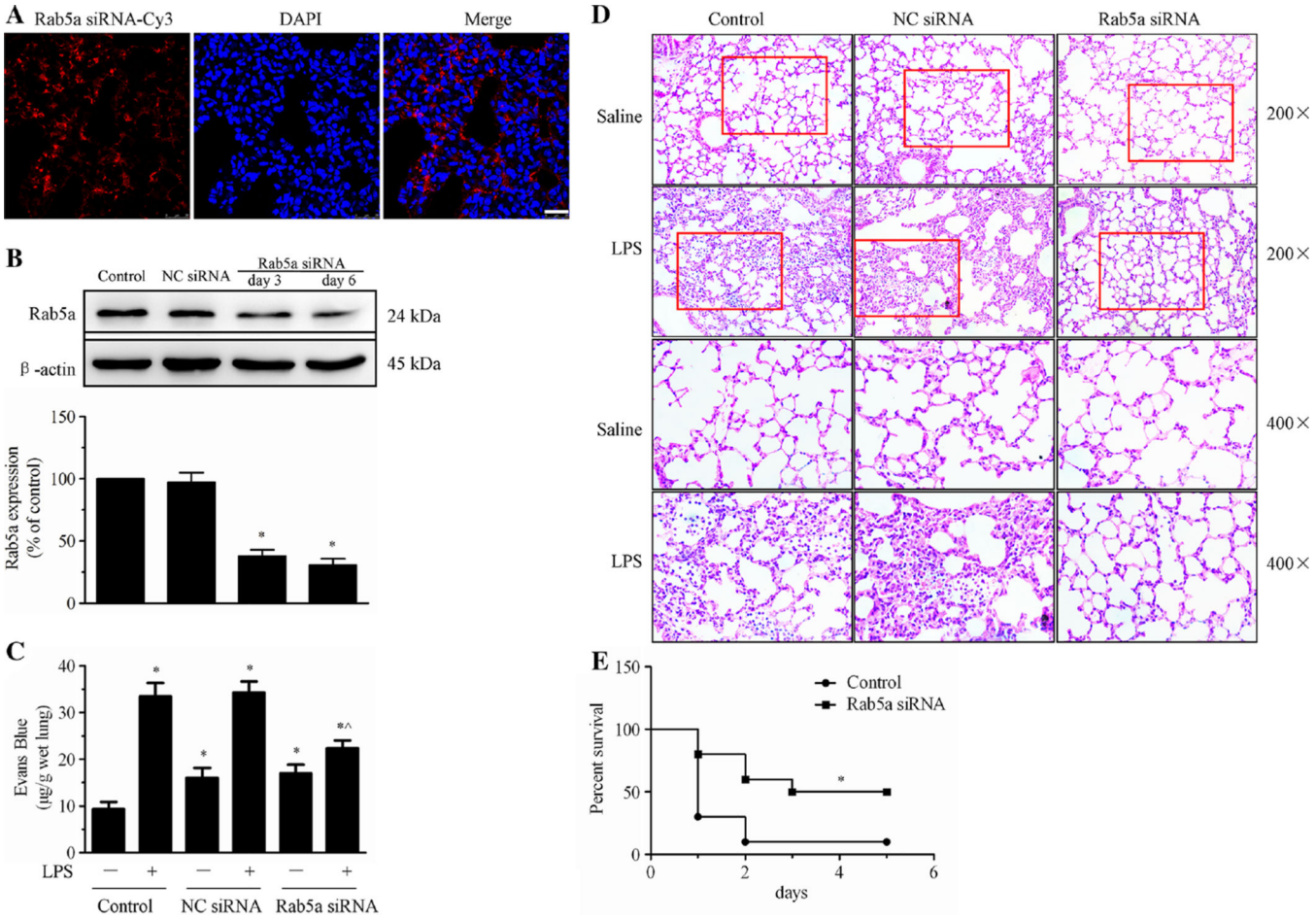

Fig. 10. Silencing Rab5a with siRNA attenuates LPS-induced endothelial barrier dysfunction in vivo

a The distribution of Cy3-tagged Rab5a siRNA in lung tissue samples isolated from C57BL/6 mice. OTC-embedded lung sections were prepared 6 days after transfection and stained with DAPI. The Cy3-expressing cells in lung tissues were visualized under a confocal microscope. *Red*, Cy3; *blue*, DAPI. *Scale bar* 25 μm. **b** Rab5a expression in lung tissues after transfection with Rab5a siRNA. C57BL/6 mice were injected via the tail vein with NC siRNA or Rab5a siRNA. Lung tissue samples were collected 3 and 6 days later. Rab5a expression was analyzed via WB. *Representative blots* showing Rab5a (*upper panel*) and β-actin expression (*lower panel*) are included. *Lower panel* shows quantitative data of Rab5a protein levels, normalized to β-actin. The data are presented as the mean ± SE $n = 3$. *$p < 0.05$ versus the control group. **c** C57BL/6 mice were injected via the tail vein with NC siRNA or Rab5a siRNA and then challenged with 20 mg/kg LPS via i.p. injection. Evans blue tracer (40 mg/kg) was injected 24 h after the LPS challenge. The lungs of the mice were harvested 2 h after Evans blue dye injection, and pulmonary transvascular permeability was measured. The data are presented as the mean ± SE, $n = 4$. *$p < 0.05$ versus the control group; ^$p < 0.05$ versus the NC siRNA plus LPS treatment group. **d** C57BL/6 mice were injected via the tail vein with NC siRNA or Rab5a siRNA, and 20 mg/kg LPS was injected 5 days after transfection. The mice were killed 24 h after LPS injection. Lung tissue samples

were fixed with 4 % paraformaldehyde, dissected, and subjected to H&E staining (original magnification ×200, ×400). **e** Mice in the control and Rab5a siRNA groups were injected with 40 mg/kg LPS i.p., and their survival was monitored. Differences in mortality were assessed using the log-rank test. The experiments were performed with ten mice in each of the two groups. $*p < 0.05$ versus the control group